Pressurized water reactor blockage—prediction of laminar flow and temperature distributions following a loss of coolant accident

P. W. Duck* and J. T. Turner†

During the unlikely occurrence of a loss of coolant accident (LOCA) in a pressurized water reactor, it has been postulated that the fuel rod cladding may swell due to the combination of a pressure differential across the cladding and the increased temperature levels in the core. In this event, adjacent fuel rods may 'balloon' until they make contact with their neighbours, leading to a reduction in subchannel flow area, subchannels of highly noncircular cross-section, and worsening heat transfer in the blocked region of the core. A particularly important measure in predicting an upper limit on the severity of this core blockage is the peripheral variation of the wall temperature for a representative blocked subchannel. This paper is concerned with the prediction of the temperature variations in the duct wall and the fluid for fully developed laminar flow. A single subchannel is modelled as a four-cusped duct, bounded by a conducting wall of constant thickness, which is subject to uniform heat flux from the fuel. Results for this idealized problem are presented for different values of the thickness and thermal conductivity of the cladding. The important wall temperature distributions have been calculated for superheated steam to cover fluid flow conditions which might be envisaged during a LOCA. Here it must be observed that two-phase flow effects are unlikely to lead to worse heat transfer than can be predicted for single-phase steam cooling. Thus, the predicted temperature variations represent an upper bound for the low Reynolds number end of the Reflood phase in the LOCA.

Keywords: *pressurized water reactor, loss of coolant accident, fully developed laminar fluid flow, cusped channel, heat transfer, fuel rod cladding*

Introduction

The present investigation of laminar flow in a cusped channel and heat transfer through the boundary walls has its origin in a situation which might arise in the event of a loss of coolant accident (LOCA) in a pressurized water reactor (PWR). Here, the increased temperature levels in the core, together with the pressure difference between the helium 'fill gas' and the core coolant (superheated steam) may combine to cause swelling of the cladding on adjacent fuel rods. Moreover, it has been suggested that the cladding could swell to such an extent that adjacent rods make contact, leading to a reduction in subchannel flow area and a worsening of the core heat transfer in the region of the blockage. The idealized, 'singly-connected', subchannel geometry then resulting is the four-cusped duct shown in Fig 1.

The effect of these local changes of shape is to produce additional resistance to the coolant flow and a redistribution of heat transfer around the boundaries of the fuel rods. Additionally, the circumferential strain associated with the ballooning may result in significant local changes in the thickness of the cladding, thereby leading to greater azimuthal variation in the wall temperature. The net result may be to produce circumferential gradients of temperature and local 'hot spots' near the lines of contact for each group of tubes.

The determination of the fuel cladding temperature under these ballooned conditions is important if the safety implications are to be fully understood; this paper is intended as a contribution to the development of such an understanding. The problem is one of conjugate heat transfer by wall conduction and forced convection to the fluid. The complex nature of this system necessitates an iterative numerical procedure.

Initially[1], it appeared that the convection problem should be amenable to solution by a well-established finite difference procedure developed principally for the study of turbulent recirculating flow. Earlier[2], an analysis for the turbulent flow in the four-cusp channel geometry was presented, the emphasis then being on the modelling of turbulence in the vicinity of the boundary and the prediction of both the axial flow and the transverse secondary components. The heat transfer description was simplified by assuming a constant wall temperature around the periphery of the subchannel at any axial location with uniform heat input axially.

In initial discussions of this problem, it became apparent that fixed wall temperature boundary conditions may conceal the importance of a peripherally varying heat transfer rate and the consequent temperature gradients in the circumferential direction. These gradients are believed to have a critical influence on the growth of the ballooned sections of the cladding since the areas for which the temperature levels are highest may either swell or burst dependent upon the prevailing conditions.

Relevant studies have been performed by Shah and London[3], and by Eckert and Irvine[4]. For the case of fully developed laminar flow in noncircular ducts, Shah and London[3] collected information for flow and heat transfer in a variety of cross-sections. They also studied the influence of different heat transfer assumptions satisfying conditions of

(i) uniform heat flux in the flow direction, combined with uniform wall temperatures at any cross-section;
(ii) uniform axial and peripheral heat flux;
(iii) uniform wall temperature.

Eckert and Irvine[4] performed a comprehensive experimental study to determine the pressure drop and heat transfer in an

* Department of Mathematics, University of Manchester, UK
† Department of Engineering, University of Manchester, UK
Manuscript received 8 July 1986 and accepted for publication on 19 December 1986

0142-727X/87/020149-07$3.00

isosceles triangular duct. For the case of uniform heat generation in the wall of the duct, they also measured the wall temperature distribution in turbulent flow and were able to obtain the peripheral distribution of local heat transfer coefficient from these data.

An interesting feature which results from these investigations[3,4] is the dependence of the mean Nusselt number on both the thermal boundary condition and the geometry of the cross-section. From Ref 3 it is clear that shapes with very sharp corners exhibit the smallest mean Nusselt numbers; thus it can be anticipated that a four-cusp duct will have characteristics in keeping with this observation. It is also to be borne in mind that the present analysis employs the more realistic convective boundary condition which results from the conjugate heat transfer problem.

While this paper deals with laminar flow heat transfer, it is pertinent to mention the inadequacy of the equivalent-diameter concept in the prediction of turbulent flow and heat transfer in noncircular ducts[2]. Again, the sharpness of any corners and their influence on the mean flow patterns must be recognized as contributing to this inadequacy.

In the following sections, a theoretical model of the fully developed laminar flow situation is introduced. Computer predictions for the heat transfer properties and flow distributions in the wall and the fluid are then presented.

Theoretical analysis

Heat transfer model of the blocked subchannel

In order to predict the surface temperature of a PWR fuel rod, the conjugate conduction and convection problem is modelled as shown in Fig 2. The fluid is assumed to be in fully developed laminar flow through the channel and to satisfy symmetry along the side and corner bisectors AB and OB, respectively. However, although the condition of uniform heat flux is imposed at the fuel–cladding interface, azimuthal heat conduction in the assumed uniformly thick cladding implies that the boundary conditions for the forced convection heat transfer are those of constant total heat flux along the axial direction with peripherally varying heat flux at the cladding–coolant interface. The temperature T within the fluid must then satisfy an expression of the form

$$T(r,\theta,z)=f_1(r,\theta)+g(z) \tag{1}$$

This paper concentrates upon the solution for $f_1(r,\theta)$ since $g(z)$ is a known linear function. The heat conduction is tacitly assumed to be one-dimensional, following the practice used in the analysis of fins. This theory is outlined in Appendix 1. It should be mentioned that circumferential variations in the wall thickness, as could be expected to occur during the ballooning process, could be easily accommodated by modifying the basic equations in the present model.

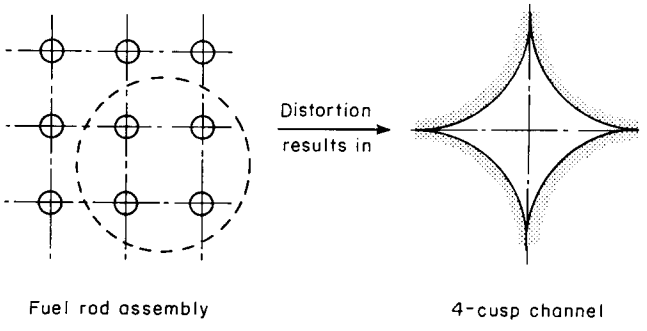

Figure 1 Origin of four-cusped channel in PWR blockage problem

Coordinate system and method of solution

A schematic diagram of the four-cusped problem is shown in Fig 1. Basically, what is required is the determination of the fluid velocity distribution in the channel, and the associated temperature fields in the fluid and the cladding. It is necessary to prescribe the geometrical and material properties of the heat flux at the fuel–cladding interface, and the axial pressure gradient. Since the temperature field (Eq (1)) is assumed to be fully developed, the temperature level of the fluid relative to the cusp remains constant for fixed values of (r,θ), irrespective of axial position.

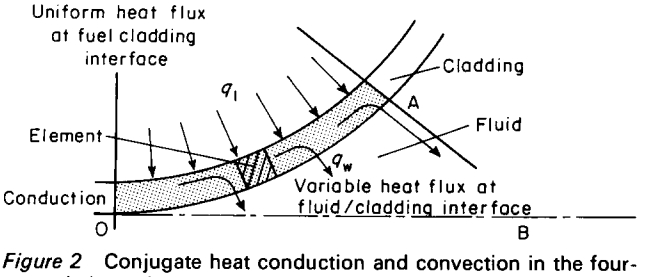

Figure 2 Conjugate heat conduction and convection in the four-cusped channel

Notation

a	External radius of cladding
b	Function in Eq (10)
C_p	Specific heat of fluid
d	Source term in Eq (10)
D_e	Equivalent diameter of noncircular channel
f	Friction factor $\equiv(\Delta p/\frac{1}{2}\rho u^2)(D_e/4L)$
$f_1(r,\theta)$	Temperature function–Eq (1)
$g(z)$	Temperature function—Eq (1)
h	Heat transfer coefficient
$H(\theta)$	Scaling function (Appendix 3)
k	Thermal conductivity
L	Length of subchannel considered
Nu	Nusselt number $\equiv hD_e/k_f$
p	Static pressure
q	Heat flux
r,θ,z	Cylindrical coordinates (radial, circumferential, axial)
$\hat{r}$	Scaled radial coordinate in transformation—Eq (2)
R	Dimensionless radial scale $\equiv r/a$
Re	Reynolds number $\equiv\rho\bar{u}D_e/\mu$
$s(\theta)$	Scaling function in transformation—Eq (2)
t	Thickness of cladding
T	Temperature
u	Velocity component in axial direction
U	Scaled velocity component in axial direction
x	Distance along cladding from cusp (Appendix 1)
α	Thermal diffusivity $\equiv k_f/\rho C_p$
Δ	Operator showing small change in value
μ	Absolute viscosity
ρ	Fluid density
Φ	Generalized dependent variable
τ	Shear stress

Subscripts

i	(Fuel/cladding) interface
w	(Flow/cladding) interface
Φ	Pertaining to variable of Φ
b	Bulk mean condition
f	Fluid
¯	Overbar denotes (area weighted) mean

Appropriate boundary conditions must be imposed in the calculation of the fluid velocity and temperature distributions within the cladding and the fluid. Additionally, the velocity and temperature fields are considered to be symmetrical about both the side bisector AB and the corner bisector OB.

In an early attempt at solution, a straightforward polar coordinate system (origin at the centre of one of the rods—see Fig 2) was employed. The attraction of this scheme was that two (of the three) boundaries of the domain of integration lay along coordinate lines (OA and AB). Unfortunately, the third boundary, OB, was not so conveniently located, and the scheme proved numerically unreliable, probably due to the poor resolution in the vicinity of the cusp where there were few mesh points.

These difficulties have been overcome by means of a modification to this scheme[5] which uses the same system of polar coordinates described above, but transformed so that all three boundaries of the integration domain lie along coordinate lines. At the same time, the new scheme gives a good mesh point distribution in the neighbourhood of the cusp.

The idea behind this coordinate system is simple. Referring to Fig 3, it can be seen that scaling of the reduced radial coordinate $(R-1)$ by the function $s(\theta)$, representing the distance at a given angular value θ between the outer surface of the cladding and the cusp bisector OA, maps the flow domain onto a rectangular region. The appropriate transformation is

$$\hat{r}=\frac{R-1}{s(\theta)} \tag{2}$$

where

$$s(\theta)=\sec\theta-1$$

This transformation maps the region inside OBA in the (r,θ) plane into the more convenient rectangular region defined by $0\leqslant\theta\leqslant\pi/4$, $0\leqslant\hat{r}\leqslant1$ in the $(\hat{r},\theta)$ plane, as shown in Fig 3. Consequently, simplification of the domain is achieved at the expense of a nonorthogonal coordinate system, with a subsequent complication in the governing equations. However, since a numerical solution is sought, this is of little concern. Special attention using this approach was required near the cusp where the cusp point 0 is mapped into the line 00′. Full details of the analysis have been given in Duck[5], and a summary of the method appears in Appendix 3.

Standard second-order central differencing was employed to approximate both the flow and energy equations, and the resulting algebraic equations were then written in tridiagonal form (along the lines of $\theta=$ constant). The equations were solved using Gaussian elimination, coupled with a standard iterative procedure.

The tolerance limit imposed on the iterative procedure was that the maximum change in any of the calculated quantities was no more than 10^{-10}, with a relaxation parameter of unity. (No optimization of this value was carried out.) Computing times on a CDC 7600 were typically of the order of 5 s, 50 s, 675 s, for a 11×11, 21×21, 41×41 grid, respectively (although these timings were dependent upon the particular problem under consideration).

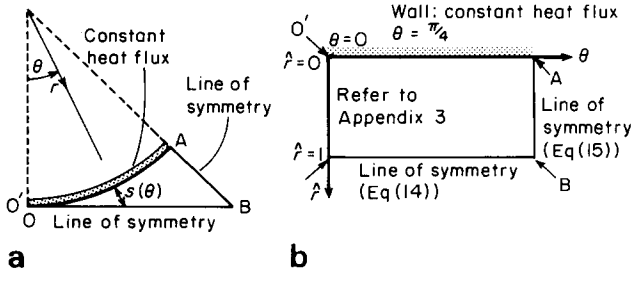

Figure 3 Coordinate system in original and transformed domains: (a) original polar coordinate scheme; (b) transformed domain

One point worth noting is that the heat transfer solution was considerably slower to converge than the corresponding flow problem. It seems likely that this discrepancy arises because the heat transfer must satisfy entirely derivative boundary conditions for the temperature, whereas, in the velocity field problem, the fluid velocity is prescribed explicitly on the walls of the cross-section.

Flow and heat transfer conditions

The problem is one of determining the fluid velocity in the channel and then matching this to the temperature fields in the fluid and the cladding. It is necessary to prescribe the geometrical and material properties, the heat flux at the fuel–cladding interface, and the axial pressure gradient in the fluid. Since the temperature field is assumed to be fully developed, it can be expressed by Eq (1), implying as stated previously that the temperature levels of the fluid relative to the cusp remain constant for fixed values of (r,θ), irrespective of the axial position.

The axial temperature gradient $(\partial T/\partial z)$, which acts as the source term for the temperature equation, equals the gradient of the bulk temperature $(\mathrm{d}T_b/\mathrm{d}z)$ for the specified thermal boundary conditions. In addition, $(\mathrm{d}T_b/\mathrm{d}z)$ is related to the boundary heat flux q_w, and the mass flow rate through the channel, by the steady flow energy equation. Fluid properties can be evaluated at the bulk temperature of the fluid.

To obtain a solution, a reference temperature value is chosen arbitrarily, and all other temperatures, both in the fluid and the cladding, are determined relative to this value. The mean fluid temperature $\bar{T}$ is calculated from the fluid temperature distribution using a numerical approximation to the equation

$$\bar{T}=\frac{\int T_f\,\mathrm{d}A}{\int \mathrm{d}A} \tag{3}$$

The local heat transfer coefficient h can then be calculated in the usual way from the difference between the wall temperature at a particular angular position and the mean temperature of the fluid, using the expression

$$h=q_w/(T_w-\bar{T}) \tag{4}$$

Here q_w is the local heat transfer to the fluid—see Appendix 1.

Results

Temperature fields in fluid and cladding

Computer predictions of the fluid velocity and temperature fields have been obtained for a four-cusp channel made up of 9.5 mm diameter fuel rods swollen to 12.6 mm diameter. These dimensions were chosen to correspond to current PWR designs[6]. For the results presented in this paper, superheated steam at 200°C and 3 bar has been considered as the coolant, corresponding to the critical period before rewetting of the cladding after the LOCA. Coupled with these fluid conditions, the temperature distribution in a segment of the cladding (OA) has been determined numerically for different assumed values of the cladding thickness, and Reynolds number. The results are presented in graphical form in Figs 4 to 9.

Fig 4 shows the temperature profile along the cladding for fixed values of the Reynolds number and thermal conductivity, but with varying thicknesses of the cladding. As expected, thinning of the cladding, such as would probably occur during the clad ballooning process in a LOCA, increases the temperature variation along the wall section.

The predicted temperature values in the duct, based upon what is clearly an idealized situation, have been obtained without any allowance for changes in the fluid properties. The calculations yield isotherms which are geometrically similar to the isovels. For the conditions specified in Table 1, a maximum temperature difference of 2400°C below the arbitrary reference

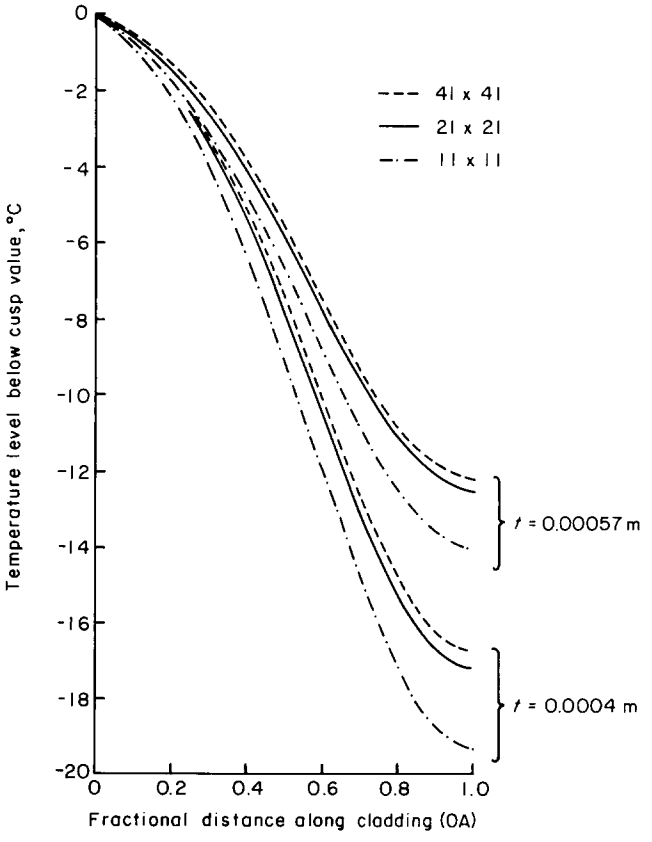

Figure 4 Peripheral variation of temperature in cladding—influence of discretization errors. k_w=19 W/(m K), q_i=18 kW/m^2, Re=10^3

Table 1 Data used as basis for calculations[6]

(i) Fuel rod surface heat flux (average)	600 kW/m^2
Decay heat during LOCA (used in calculation)	18 kW/m^2
(ii) Fuel rod dimensions: swollen outer diameter	12.6 mm
cladding thickness	0.57 mm
(iii) Zircalloy cladding: conductivity k_w	19 W/(m K)
(iv) Steam conditions: specific heat C_p	1.94 kJ/(kg K)
dynamic viscosity μ_f	16.2×10^{-6} kg/(m s)
conductivity k_f	33.2×10^{-3} W/(m K)

level (at the cusp) is calculated at the centre of the duct (point B). This is obviously unrealistic and reflects the arbitrary choice of parameters in which a high heat input, corresponding to 3% of the design power level, has been assumed. The actual temperature at any axial station may then be obtained by superposition, combining the computed temperatures (relative to the cusp) with the axial gradient of the bulk temperature (dT_b/dz) and the chosen location z—see Eq (1).

The maximum value of the temperature difference around the cladding is of immediate interest in safety studies. This value has been plotted in Fig 5 corresponding to the conditions specified in Table 1 except for the cladding thickness, which has been varied systematically. The results confirm the expected trends of increasing temperature difference as the cladding thickness decreases. Perhaps it should also be observed that experimental study[7] of the flow in a four-cusped channel has suggested transition Reynolds numbers lying between 1800 and 2000. Thus, the Reynolds number values considered in the present numerical study (of order 1000) are appropriate to the assumed laminar flow conditions.

Although there are other obvious parameters, such as the wall conductivity k_w, controlling the temperature variation in the cladding, in the context of PWR design the thermal conductivity value taken here is the most realistic, since Zircalloy is currently the preferred cladding material in all PWR designs. It is then apparent that the most significant influence on the wall temperature variations will be the decrease in cladding thickness as the ballooning process proceeds.

The velocity field

This study has been primarily concerned with heat transfer aspects of the PWR blockage problem, even though these cannot be determined without initially solving for the fluid velocity field. As part of the computer program, therefore, the friction factor was determined from the specified axial pressure gradient and the average velocity for the section (yielded by the computer solution). Furthermore, since laminar flow was studied, the local shear stress on the cladding could be estimated from the velocity gradient normal to the wall, and the absolute viscosity. This enabled a check to be made to ensure compatibility between the predicted friction factor and the measured correlation[8].

Fig 6 shows the velocity field within the four-cusp channel in terms of the contours of constant velocity level. Note that these values were computed for a specified pressure gradient. The

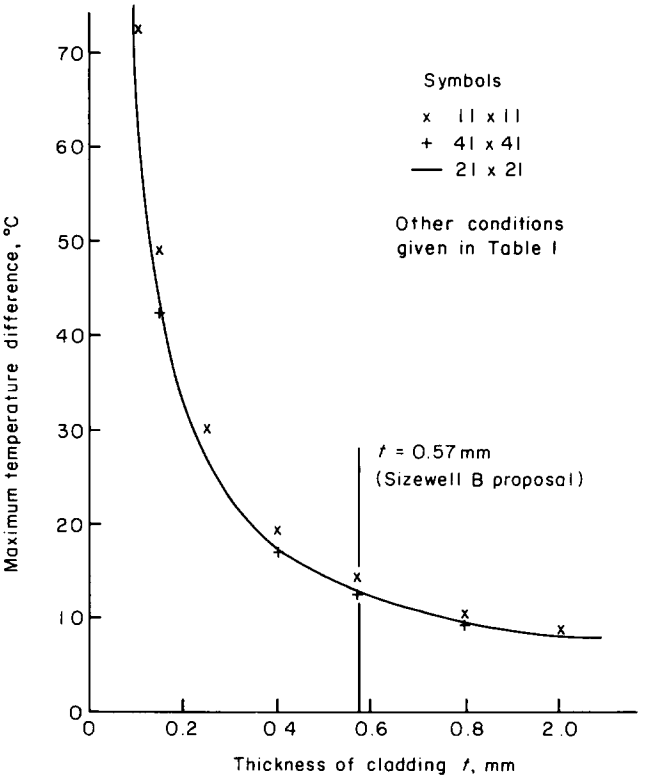

Figure 5 Maximum temperature difference in cladding—influence of discretization errors

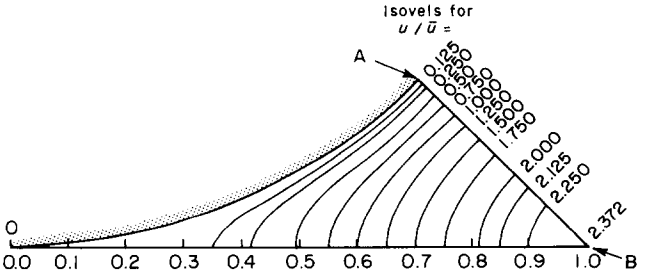

Figure 6 Isovels in one half quadrant of duct

velocity variation along the lines OB and OA is then shown as Fig 7. Subsequently, the velocity field yields the distribution of the wall shear stress τ_w, rendered dimensionless by the mean value $\bar{\tau}_w$, as presented in Fig 8. Figs 6, 7 and 8 reflect the way in which the cusped wall junction produces a substantial region of low energy fluid in the corners.

In some experiments to determine the dependence of the friction factor on the Reynolds number for a four-cusped channel, Haque[8] found that

$$f = 6.5/Re \tag{5}$$

This value should be contrasted with the computed result obtained here using a numerical approximation to the expression for the average shear stress along the cladding surface,

$$\bar{\tau}_w = \int_0^{\pi/4} \tau_w \, d\theta/(\pi/4) \tag{6}$$

Converting this into a friction factor yields a result for the product $fRe = 6.62$. This satisfactory agreement is reassuring.

Heat transfer to the fluid

The heat transfer coefficient defined by Eq (4) is easily calculated from the temperature variations in the fluid. Then the local heat

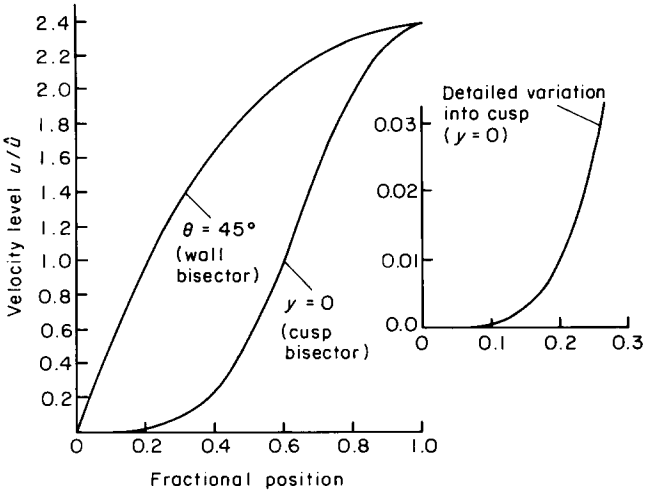

Figure 7 Velocity distribution across channel. Detail shows quality of convergence achieved

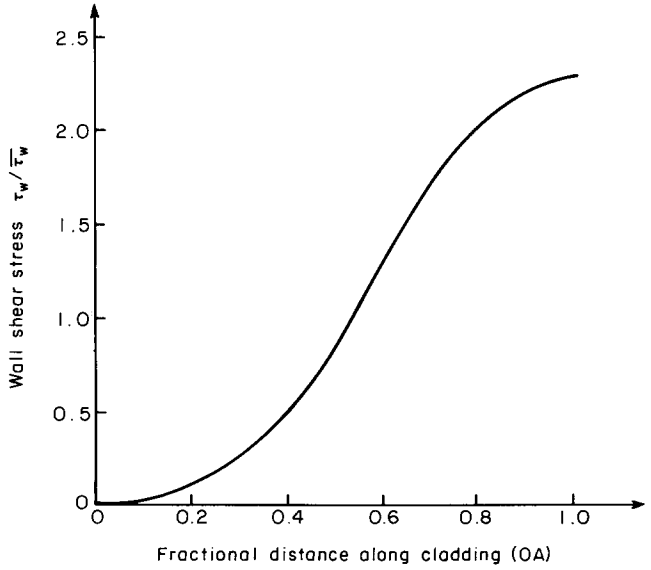

Figure 8 Peripheral variation of wall shear stress. NB: Mean wall shear stress $\bar{\tau}_w = \mu(\partial u/\partial r)_w$ obtained by integration around surface (Eq (6))

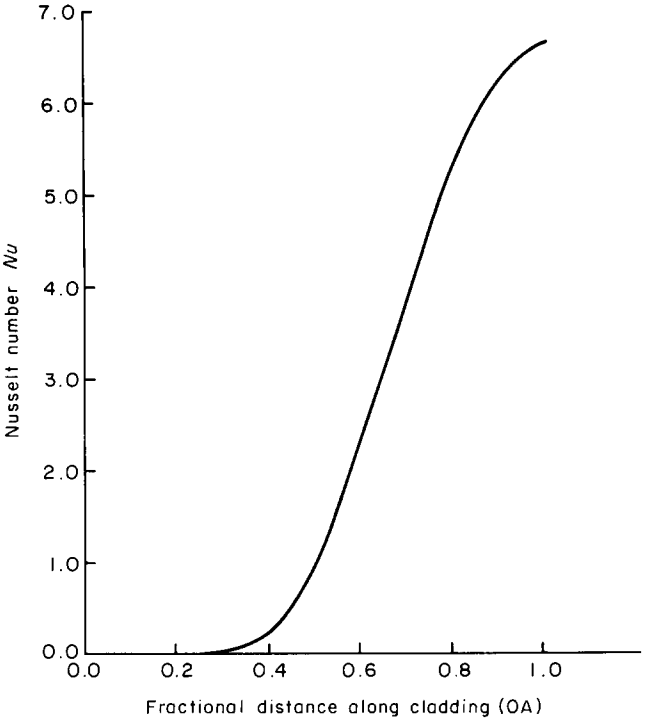

Figure 9 Peripheral variation of Nusselt number (NB: independent of Reynolds number)

Table 2 Mean Nusselt number as a function of cladding thickness, based on 21 × 21 results

Wall thickness t (mm)	0.15	0.40	0.80
Mean Nusselt number $\bar{Nu}$	2.185	2.180	2.172

transfer coefficient h can be integrated around the cladding surface to determine the average coefficient $\bar{h}$ using a numerical approximation to the expression

$$\bar{h} = \int_0^{\pi/4} h \, d\theta/(\pi/4) \tag{7}$$

Thus the local and mean values of the Nusselt number can be determined, leading to the results which are summarized in Fig 9 and Table 2. It is interesting to observe that changing the thickness t of the cladding produces less than one percent variation in the local Nusselt number, as represented by the curve in Fig 9. Similarly, the surface-averaged Nusselt number $\bar{Nu}$ changes only very slightly when the cladding thickness is altered from 0.8 mm to 0.15 mm. Such changes are insignificant in view of the other major assumptions in the analysis.

Following normal practice, it is likely that the $\bar{Nu}$ value could be assumed to apply for different boundary conditions at the surface (eg variable heat flux in the azimuthal direction). Although no empirical data appear to be available for a four cusped channel, Shah and London[3] have presented a table of heat transfer data for other noncircular ducts. The computed values obtained here are in broad agreement with these data and are independent of the Reynolds number assumed, because of the way in which the problem is posed.

More realistic modelling

In the event of a LOCA, distortion of the fuel elements by ballooning would produce a space between the fuel pellets and the cladding. In turn, this would lead to variable heat flux (by radiation) at the inner surface of the cladding and

circumferential variations in the thickness of the cladding. Such additional complications could easily be included in the numerical scheme by introducing an angular dependence for the terms q_i and t as explained in Appendix 1.

Current thinking appears to couple the four-cusped channel shape with decreasing cross-sectional area along the flow direction. Hence, the real problem becomes one of accelerating flow through the subchannel, with variable heat flux into the cladding. These modifications, which must influence the velocity and temperature fields in the fluid, and the temperature distribution around the cladding, are currently receiving attention.

Conclusion

A numerical procedure has been described which enables the temperature attained by swollen PWR fuel rod cladding to be determined. The problem solved is that of conjugate conduction through the cladding, coupled with laminar convection into the fluid; a four-cusp cross-sectional shape is assumed for the flow channel. Constant heat flux at the fuel–cladding interface, laminar flow conditions, and fully developed but uncoupled velocity and temperature fields are assumed in formulating the problem. Only small changes to the computational procedures would be needed to accommodate variable heat flux from the fuel to the cladding. The method could be extended to other geometries with relative ease.

Results have been presented for the temperature variation in the cladding, the heat transfer coefficient, the fluid velocity and temperature fields, and the surface shear stress distribution. Excellent agreement is found between the computed values for the friction factor and the mean Nusselt number, and the limited data available in the literature.

Acknowledgement

During the early stages of this study, considerable help in formulating the problem was received from Dr. H. Barrow of the University of Liverpool. This assistance is greatly appreciated.

Some of the work described in this paper was supported financially by the Health and Safety Executive as part of the research programme of HM Nuclear Installations Inspectorate. The authors are grateful for this support but wish to state that the views expressed here are their own and do not necessarily represent those of the sponsors.

References

1 Gosman, A. D., Pun, W. M., Runchal, A. K., Spalding, D. B. and Wolfshtein, M. *Heat and Mass Transfer in Recirculating Flows*, Academic Press, London and New York, 1969

2 Haque, M. A., Hassan, A. K. A., Turner, J. T. and Barrow, H. The prediction of forced convection in a cusp shaped channel. 7th Int. Heat Transfer Conf., Munich, 1982

3 Shah, R. K. and London, A. L. *Laminar Forced Convection in Ducts*, Academic Press, 1978

4 Eckert, E. R. G. and Irvine, T. F. Pressure drop and heat transfer in a duct with triangular cross section. *J. Heat Trans., Trans. ASME*, 1960, 125–138

5 Duck, P. W. Submitted to the *Int. J. Heat Mass Transfer*

6 *Design data for Sizewell B Pressurised Water Reactor*, CEGB, 1984

7 Turner, J. T. and Haque, M. A. PWR blockage: an experimental study of fluid flow and heat transfer in a model core. *Proc. I. Mech. E.*, 1983

8 Haque, M. A. An experimental and computational study of the PWR blockage problem, PhD Thesis, University of Manchester, 1984

9 Hornby, R. P. and Barrow, H. A compatibility error in the formulation of a popular general purpose finite difference scheme for the solution of elliptic partial differential equations. *Int. J. Heat and Fluid Flow*, 1979, **1**(1), 13–16

Appendix 1: Thermal conduction in the fuel rod cladding

The model for the thermal conduction in the cladding material is shown in Fig 10. Unidirectional heat conduction is assumed, following the practice adopted in fin theory. Although the analysis applies to cladding with circumferentially varying thickness, it can be simplified for the case presented in this paper.

An energy balance for the element of the cladding results in

$$\left(1-\frac{t}{a}\right)q_i = -k_w t\frac{\partial^2 T}{\partial x^2} - k_w\frac{\partial t}{\partial x}\frac{\partial T}{\partial x} + q_w \tag{8}$$

provided that axial heat conduction is ignored.

Thus, for the particular case where the cladding is of constant thickness

$$\left(1-\frac{t}{a}\right)q_i = -k_w t\frac{\partial^2 T}{\partial x^2} + q_w$$

and

$$q_w = -k_f\left(\frac{\partial T}{\partial r}\right)_w \tag{9}$$

This equation must be satisfied simultaneously with the energy equation for the fluid. For this purpose, the equation is written in finite difference form and solved together with the convection equations discussed in Appendix 2. The fuel–cladding interface heat flux q_i needs to match the specified axial temperature gradient in the fluid. For the assumed fully developed temperature conditions, this temperature gradient will be constant. This latter constraint is enforced once the velocity field and, hence, mass flowrate have been obtained for the specified axial pressure gradient. An overall energy balance for the cladding–fluid control volume relates the heat flux q to the axial enthalpy increase of the fluid.

The peripheral temperature gradients in the cladding at O and A are zero because of symmetry; these conditions are accommodated in the usual way in the numerical method. In practice, Eq (9) could be developed further to cater for two-dimensionality. However, since the thickness of the cladding is small compared with its radius, these effects are relatively insignificant.

Appendix 2: Analysis of laminar flow distribution and heat transfer by forced convection

The momentum and energy equations for fully developed steady laminar flow in the channel may be written in a generalized

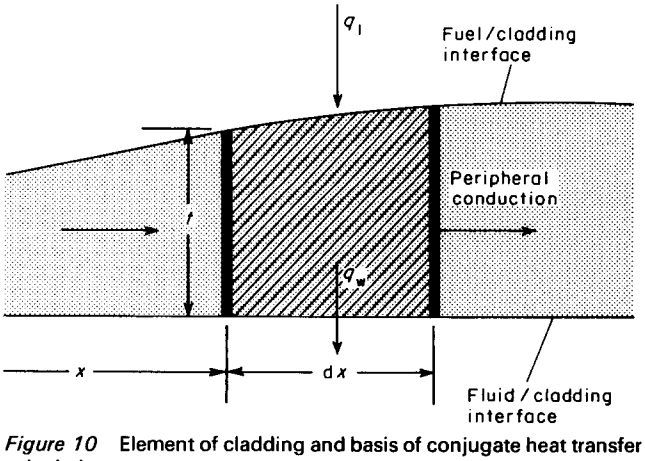

Figure 10 Element of cladding and basis of conjugate heat transfer calculations

Table 3 Meanings of quantities in Eq (10)

Φ	b_Φ	d_Φ (source)
u	1	$\frac{1}{\mu}\frac{\partial p}{\partial z}$
T	1	$\frac{u}{\alpha}\frac{\partial T}{\partial z}$

form, following Gosman *et al*[1], as

$$-\frac{\partial}{\partial r}\left(rb_\Phi\frac{\partial\Phi}{\partial r}\right)-\frac{\partial}{\partial\theta}\left(\frac{1}{r}b_\Phi\frac{\partial\Phi}{\partial\theta}\right)+rd_\Phi=0 \tag{10}$$

Here, the various quantities have the meanings listed in Table 3.

The boundary conditions for the velocity and temperature are briefly discussed in the second section of the paper, particular attention being given to the attainment of symmetry along the cusp bisector OB. Along the cladding–fluid interface, the velocity is everywhere zero while the temperature there is made compatible with the heat conduction in the cladding (see Appendix 1).

Noting that laminar flow is assumed, the axial pressure gradient ($\partial p/\partial z$) has to be chosen accordingly. An estimate of this quantity is made using the appropriate relationship for frictional pressure drop in laminar flow given in Turner and Haque (1983); thus the velocity level can be determined. Further integration yields the mean velocity and permits the Reynolds number to be evaluated.

Appendix 3: System of coordinates

As noted in the second section of the paper, an early approach to both the flow and heat transfer patterns involved the use of polar coordinates $r(,\theta)$, but this proved unreliable. Instead, an approach involving nonorthogonal coordinates (for full details see Duck[5]) was adopted. In this paper, details will only be given for the flow problem; the technique used to determine the heat transfer solution is virtually identical.

A scaled radial coordinate $\hat{r}$ is used, as defined by Eq (2), whilst the angular coordinate θ is left unchanged. It is also found convenient to work with a scaled velocity field $U(\hat{r},\theta)$, defined by

$$u=U(\hat{r},\theta)H(\theta) \tag{11}$$

Substitution of this into the fully developed momentum equation (10) yields the following partial differential equation for U:

$$\left[\frac{H}{s^2}+\frac{H\hat{r}^2s'^2}{s^2(1+s\hat{r})^2}\right]\frac{\partial^2U}{\partial\hat{r}^2}+\left[\frac{H}{s(1+s\hat{r})}+\frac{1}{(1+s\hat{r})^2}\left(\frac{2\hat{r}s'^2H}{s^2}-\frac{s\hat{r}s''H}{s}-\frac{s\hat{r}s'^2H}{s}\right)\right]\frac{\partial U}{\partial\hat{r}}$$
$$+\frac{H''}{(1+s\hat{r})^2}U+\frac{2H'}{(1+s\hat{r})^2}\frac{\partial U}{\partial\theta}+\frac{H}{(1+s\hat{r})^2}\frac{\partial^2U}{\partial\theta^2}$$
$$-\frac{2\hat{r}s'H}{s(1+s\hat{r})^2}\frac{\partial^2U}{\partial\hat{r}\,\partial\theta}=\frac{a^2}{\mu}\frac{\partial p}{\partial z} \tag{12}$$

There is now a rectangular grid on which to compute, and so the boundary conditions may be enforced rather more easily. Along the boundary $\hat{r}=0$, there is the condition of no slip, namely

$$U(0,\theta)=0, \qquad 0\leqslant\theta\leqslant\pi/4 \tag{13}$$

On two of the other edges of the computational domain, symmetry must be imposed. This requires that

$$-\frac{H}{s}\frac{\partial U}{\partial\hat{r}}\cos\theta+\frac{\sin\theta}{1+s}\left(H\frac{\partial U}{\partial\theta}+H'U-\frac{s'H}{s}\frac{\partial U}{\partial\hat{r}}\right)=0 \tag{14}$$

$$\text{on } \hat{r}=1, \qquad 0\leqslant\theta\leqslant\frac{\pi}{4}$$

together with

$$H\frac{\partial U}{\partial\theta}+H'U-\frac{\hat{r}s'H}{s}\frac{\partial U}{\partial\hat{r}}=0 \tag{15}$$

$$\text{on } \theta=\pi/4, \text{ for } 0\leqslant\hat{r}\leqslant1$$

Before specifying the boundary condition on the fourth edge of the domain, the scaling factor H must first be specified. Following Duck[5], this was taken to be

$$H=s^2(\theta) \tag{16}$$

The choices of H and $s(\theta)$ reflect the local behaviour of the solution close to a cusp, as detailed in Ref 5. With this, the fourth boundary condition becomes

$$U=\tfrac{1}{2}\hat{r}^2-\hat{r} \tag{17}$$

$$\text{for } \theta=0, \ 0\leqslant\hat{r}\leqslant1$$

This completes the solution for the axial fluid velocity. In the case of the heat transfer problem, the primary difference in the approach was that H was taken to be unity (to reflect the local behaviour of the temperature close to the cusp), and the boundary condition on the temperature on this fourth edge was taken to be

$$T=\text{constant } (=0, \text{ say}) \tag{18}$$

$$\text{for } \theta=0, \ 0\leqslant\hat{r}\leqslant1$$